obtained by dissecting hypothalamic wedges (containing ventromedial and arcuate nuclei) from 350-μm hypothalamic slices and incubating in 10 ml of 1 mg ml^{-1} protease (Type XIV, Sigma) in aCSF equilibrated with 95% O_2, 5% CO_2, at room temperature for 1 h, followed by washing 5 times with 30 ml aCSF. The wedges were resuspended in aCSF (10 ml) and dissociated by gentle trituration. Dissociated neurons were plated into tissue-culture dishes containing 1 ml of normal saline and 10 mM glucose and left for 20 min before patching. Recordings were made using an Axopatch 200A patch-clamp amplifier at room temperature with patch-pipettes (5–10 MΩ) filled with the following solution (in mM): KCl 140, $CaCl_2$ 1, $MgCl_2$ 1, HEPES 10, pH 7.2; and for some outside-out recordings, KCl 140, $CaCl_2$ 3.25, $MgCl_2$ 1, EGTA 10, Mg-ATP 2, HEPES 10, pH 7.2 (free Ca^{2+} of 100 nM). The bath solution (normal saline) consisted of (in mM): NaCl 135, KCl 5, $CaCl_2$ 1, $MgCl_2$ 1, HEPES 10, Glucose 3, pH 7.4 with NaOH; for current–voltage relations during inside-out recordings, KCl 140, $CaCl_2$ 9.75, $MgCl_2$ 1, EGTA 10, HEPES 10, pH 7.2 (free Ca^{2+} of 10 μM). Data were displayed on a chart recorder (Gould Easygraph), and stored on DAT for off-line analysis. The potential across the membrane is described following the usual sign convention for membrane potential (inside negative). Outward current is shown as upward deflections on all single-channel records. The data were analysed for current amplitude and average activity (N_tP_o) as described previously[30]. ATP (Sigma) was made up as a 100-mM stock solution in 10 mM HEPES, pH 7.2, and kept at −4 °C until required. Tolbutamide and leptin were made up and applied to the bath as described above. Significance levels in all cases were determined by Student's *t*-test. Results are expressed as the mean ± s.e.m.

Received 2 June; accepted 15 September 1997.

1. Caro, J. F., Sinha, M. K., Kolaczynski, J. W., Zhang, P. L. & Considine, R. V. Leptin: The tale of an obesity gene. *Diabetes* **45,** 1455–1462 (1996).
2. Matson, C. A., Wiater, M. F. & Weigle, D. S. Leptin and the regulation of body adiposity. *Diabetes Rev.* **4,** 488–508 (1996).
3. Stephens, T. W. *et al.* The role of neuropeptide Y in the antiobesity action of the *obese* gene product. *Nature* **377,** 530–532 (1995).
4. Satoh, N. *et al.* The arcuate nucleus as a primary site of satiety effect of leptin in rats. *Neurosci. Lett.* **224,** 149–152 (1997).
5. Vaisse, C. *et al.* Leptin activation of Stat3 in the hypothalamus of wild-type and *ob/ob* mice but not *db/db* mice. *Nature Genet.* **14,** 95–97 (1996).
6. Levin, B. E. & Routh, V. H. Role of the brain in energy balance and obesity. *Am. J. Physiol.* **40,** R491–R500 (1996).
7. Zhang, Y. R. *et al.* Positional cloning of the mouse *obese* gene and its human homologue. *Nature* **372,** 425–432 (1994).
8. Lee, G.-H. *et al.* Abnormal splicing of the leptin receptor in *diabetic* mice. *Nature* **379,** 632–635 (1996).
9. Chen, H. *et al.* Evidence that the diabetes gene encodes the leptin receptor: Identification of a mutation in the leptin receptor gene in db/db mice. *Cell* **84,** 491–495 (1996).
10. Chua, S. C. Jr *et al.* Phenotypes of mouse *diabetes* and rat *fatty* due to mutations in the OB (leptin) receptor. *Science* **271,** 994–996 (1996).
11. Oomura, Y., Ono, T., Ooyama, H. & Wayner, M. J. Glucose and osmosensitive neurones in the rat hypothalamus. *Nature* **222,** 282–284 (1969).
12. Ashford, M. L. J., Boden, P. R. & Treherene, J. M. Glucose-induced excitation of hypothalamic neurones is mediated by ATP-sensitive K^+ channels. *Pflügers Arch.* **415,** 479–483 (1990).
13. Ashford, M. L. J., Boden, P. R. & Treherne, J. M. Tolbutamide excites rat glucoreceptive ventromedial hypothalamic neurones by indirect inhibition of ATP-K^+ channels. *Br. J. Pharmacol.* **101,** 531–540 (1990).
14. Streamson, C. *et al.* Phenotype of *fatty* due to Gln269Pro mutation in the leptin receptor (*Lepr*). *Diabetes* **45,** 1141–1143 (1996).
15. Phillips, M. S. *et al.* Leptin receptor missense mutation in the *fatty* Zucker rat. *Nature Genet.* **13,** 18–19 (1996).
16. Rosenblum, C. I. *et al.* Functional STAT 1 and 3 signalling by the leptin receptor (OB-R); reduced expression of the fatty leptin receptor in transfected cells. *Endocrinology* **137,** 5178–5181 (1996).
17. Yamashita, T., Murakami, T., Iida, M., Kuwajima, M. & Shima, K. Leptin receptor of Zucker fatty rat performs reduced signal transduction. *Diabetes* **46,** 1077–1080 (1997).
18. Treherne, J. M. & Ashford, M. L. J. Calcium-activated potassium channels in rat dissociated ventromedial hypothalamic neurones. *J. Neuroendocrinol.* **3,** 323–329 (1991).
19. Tartaglia, L. A. *et al.* Identification and expression cloning of a leptin receptor, OB-R. *Cell* **83,** 1263–1271 (1995).
20. Rock, F. L., Peterson, D., Weig, B. C., Kastelein, R. A. & Bazan, J. F. Binding of leptin to the soluble ectodomain of recombinant leptin receptor. *Horm. Metab. Res.* **28,** 748–750 (1996).
21. Glaum, S. R. *et al.* Leptin, the *Obese* gene product, rapidly modulates synaptic transmission in the hypothalamus. *Mol. Pharmacol.* **50,** 230–235 (1996).
22. Mercer, J. G. *et al.* Localization of leptin receptor mRNA and the long form splice variant (Ob-Rb) in mouse hypothalamus and adjacent brain regions by in situ hybridization. *FEBS Lett.* **387,** 113–116 (1996).
23. Schwartz, M. W., Seeley, R. J., Campfield, L. A., Burn, P. & Baskin, D. G. Identification of targets of leptin action in rat hypothalamus. *J. Clin. Invest.* **98,** 1101–1106 (1996).
24. Woods, A. J. & Stock, M. J. Leptin activation in hypothalamus. *Nature* **381,** 745 (1996).
25. Elmquist, J. K., Ahima, R. S., Maratos-Flier, E., Flier, J. S. & Saper, C. B. Leptin activates neurons in ventrobasal hypothalamus and brainstem. *Endocrinology* **138,** 839–842 (1997).
26. Cusin, I., Rohner-Jeanrenaud, F., Sticker-Krongrad, A. & Jeanrenaud, B. The weight-reducing effect of an intracerebroventricular bolus injection of leptin in genetically obese fa/fa rats: reduced sensitivity compared with lean animals. *Diabetes* **45,** 1446–1450 (1996).
27. Seeley, R. J. *et al.* Intraventricular leptin reduces food intake and body weight of lean rats but not obese Zucker rats. *Horm. Metab. Res.* **28,** 664–668 (1996).
28. Keiffer, T. J., Heller, R. S., Leech, C. A., Holz, G. G. & Habener, J. F. Leptin suppression of insulin secretion by the activation of ATP-sensitive K^+ channels in pancreating β-cells. *Diabetes* **26,** 1087–1093 (1997).
29. Harvey, J., McKenna, F., Herson, P. S., Spanswick, D. & Ashford, M. L. J. Leptin activates ATP-sensitive potassium channels in the rat insulin secreting cell line, CRI-G1. *J. Physiol. (Lond.)* **504,** 527–535 (1997).
30. Lee, K., Rowe, I. C. M. & Ashford, M. L. J. Characterization of an ATP-modulated large conductance Ca^{2+}-activated K^+ channel present in rat cortical neurones. *J. Physiol. (Lond.)* **488,** 319–337 (1995).

Acknowledgements. We thank K. Todd for technical assistance. This work was supported by grants from the Wellcome Trust and Pharmacia-Upjohn.

Correspondence and requests for materials should be addressed to M.L.J.A. (e-mail: mike.ashford@abdn.ac.uk).

RGS8 accelerates G-protein-mediated modulation of K^+ currents

Osamu Saitoh*, Yoshihiro Kubo†, Yoshihide Miyatani*, Tomiko Asano‡ & Hiroyasu Nakata*

** Department of Molecular and Cellular Neurobiology, † Department of Neurophysiology, Tokyo Metropolitan Institute for Neuroscience, 2-6 Musashidai, Fuchu-shi, Tokyo 183, Japan*

‡ Department of Biochemistry, Institute for Developmental Research, Aichi Human Service Center, Kasugai, Aichi 480-03, Japan

Transmembrane signal transduction via heterotrimeric G proteins is reported to be inhibited by RGS (regulators of G-protein signalling) proteins[1–4]. These RGS proteins work by increasing the GTPase activity of G protein α-subunits (Gα), thereby driving G proteins into their inactive GDP-bound form[5–7]. However, it is not known how RGS proteins regulate the kinetics of physiological responses that depend on G proteins. Here we report the isolation of a full-length complementary DNA encoding a neural-tissue-specific RGS protein, RGS8, and the determination of its function. We show that RGS8 binds preferentially to the α-subunits Gαo and Gαi3 and that it functions as a GTPase-activating protein (GAP). When co-expressed in *Xenopus* oocytes with a G-protein-coupled receptor and a G-protein-coupled inwardly rectifying K^+ channel (GIRK1/2), RGS8 accelerated not only the turning off but also the turning on of the GIRK1/2 current upon receptor stimulation, without affecting the dose–response relationship. We conclude that RGS8 accelerates the modulation of G-protein-coupled channels and is not just a simple negative regulator. This property of RGS8 may be crucial for the rapid regulation of neuronal excitability upon stimulation of G-protein-coupled receptors.

To identify RGS proteins specifically expressed in neural cells, we used the polymerase chain reaction (PCR) on cDNA from neuronally differentiated P19 mouse embryonal carcinoma cells[8], with degenerate oligonucleotide primers corresponding to the conserved region (RGS domains) of known RGS proteins[3]. Three genes that encode RGS domains were isolated and identified as *RGS-r* (ref. 9), *RGS2* (refs 4, 10) and *RGS8* (ref. 3), respectively. We next investigated messenger RNA expression for these three RGS proteins in undifferentiated and neuronally differentiated P19 cells by reverse transcription-PCR (RT-PCR) analysis. Although expression of RGS2 and RGS-r mRNA was similar in both types of cell, that of RGS8 mRNA was significantly higher in differentiated cells (Fig. 1a).

As only a partial cDNA fragment of RGS8 has been isolated[3], we screened a rat hippocampus cDNA library with a PCR-amplified fragment of RGS8 in order to isolate a full-length cDNA clone for functional analysis. The isolated cDNA encoded a protein of 180 amino acids (Fig. 1b). Comparison of the predicted full-length amino-acid sequence with the GenBank data base revealed significantly similarity with several members of the RGS family. The predicted amino-acid sequence was identical to the partial sequence reported for RGS8 (ref. 3). Northern blot analysis indicated that

RGS8 was expressed at high levels in rat brain and barely at all in other tissues (Fig. 1c). A smaller transcript was detected in testis by the RGS8 probe (Fig. 1c, lane 8). During brain development, expression of RGS8 was detectable in 13-day-old embryos, increasing gradually in later embryos and then markedly in neonates to adults (Fig. 1d).

We next determined the specificity of RGS8 by *in vitro* binding[6]. Hexa-histidine tagged RGS8 (His-tagged RGS8) was incubated with rat brain membrane fractions treated with GDP and AlF_4^-, as other RGS proteins are known to have stronger binding to G proteins in the presence of GDP and AlF_4^- (ref. 6). Complexes containing the His-tagged RGS8 were purified on Ni^{2+}-NTA–agarose and were analysed by SDS–polyacrylamide gel electrophoresis (SDS–PAGE). After Coomassie blue staining, a protein of relative molecular mass 40,000 (M_r 40K) recovered with RGS8 (Fig. 2a). By immunoblotting using antisera specific for different subtypes of Gα subunit, we found that Gαo and Gαi3 were selectively recovered with RGS8. Only weak signals were visible for Gαi 1 and 2, Gαz and Gαq/11 (Fig. 2b). Reconstitution studies have shown that RGS proteins (RGS1, 4, 10 and GAIP) interact selectively with the Gi class of Gα subunits but that they do not discriminate individual Gαi subtypes[5–7]. Our results show that RGS8 interacts selectively with Gαo and Gαi3 in brain membranes where various subtypes of Gα exist.

To investigate how RGS8 regulates the function of Gα subunits, we tested the effects of RGS8 on the GTP hydrolysis rate of Gαo and on the GDP–GTP exchange rate of Gαo. The GTP hydrolysis rate was measured by first making GTP bind to Gαo under conditions in which the nucleotide cannot be hydrolysed, so that the GDP–GTP exchange did not limit the rate. RGS8 markedly increased the rate of GTP hydrolysis of bovine Gαo, whereas boiled RGS8 had no effect (Fig. 3a). These results indicate that RGS8 functions as a GAP for Gαo. The GDP–GTP exchange rate of Gαo was estimated by measuring the steady-state GTP hydrolysis rate, which is limited not by the rate of catalysis but by the slow exchange of GDP and GTP. RGS8 did not significantly affect the GDP–GTP exchange rate under these conditions (Fig. 3b). However, as the estimation of GDP–GTP exchange rate here was done in the absence of stimulation by an activated receptor, it remains to be seen whether RGS8 alters the fast GDP–GTP exchange rate on Gαo upon stimulation by receptor. As this step is probably too fast to be analysed biochemically, we decided to examine the kinetics of the response upon receptor activation by using electrophysiological recording.

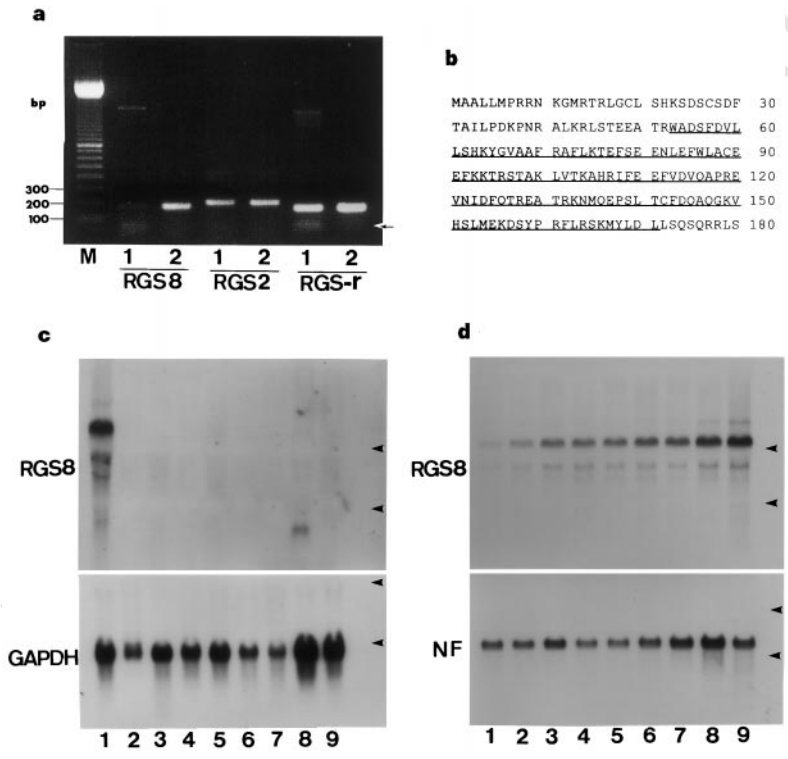

Figure 1 Detection and characterization of RGS8. **a**, Expression of RGS8, RGS2 and RGS-r during neural differentiation of P19 cells. Expression of RGS8, RGS2 and RGS-r in undifferentiated (lane 1) and neuronally differentiated (lane 2) P19 cells was examined by using RT-PCR; the position of the primers is indicated by an arrow. DNA size markers (100-bp ladder) are also shown (M). The expected size of the PCR product is ~200 bp. **b**, Amino-acid sequences of rat RGS8; the RGS domain is underlined. **c**, Northern blot analysis of various rat tissues. Lanes: 1, brain; 2, heart; 3, lung; 4, stomach; 5, spleen; 6, liver; 7, kidney; 8, testis; and 9, back muscle (M. latissimus dorsi). Total RNA (20 μg) was electrophoresed, transferred and then hybridized with full-length rat RGS8 cRNA (top) or mouse glyceraldehyde 3-phosphate dehydrogenase (GAPDH) cDNA (bottom). **d**, Northern blot analysis of RNA from developing brain. Lanes: 1, heads of 13-d embryos; 2–6, brains from 14-d, 15-d, 17-d, 19-d, 21-d embryos, respectively; 7, 8, brains from 6-d, 13-d neonates; and 9, adults. Total RNA (10 μg) was electrophoresed, transferred and then hybridized with full-length rat RGS8 cRNA (top) or mouse neurofilament (NF140K) cDNA (bottom). Probes for GAPDH and NF140K have been described[24]. Arrowheads, migration positions of 28S and 18S rRNA markers.

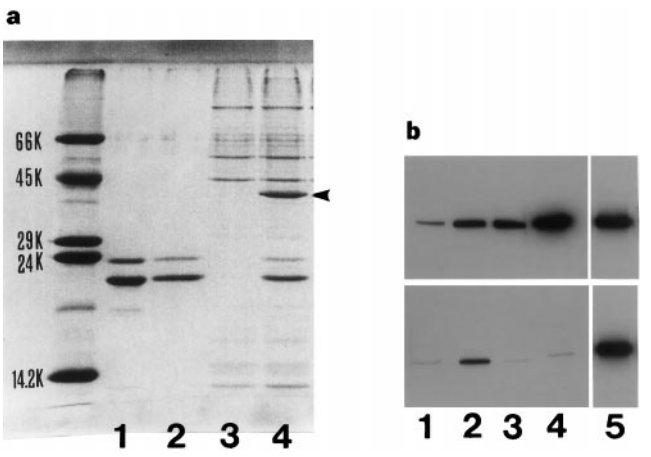

Figure 2 Interaction of RGS8 with Gα subunit. His-tagged RGS8 was incubated with rat brain membranes treated with GDP and AlF_4^-. After extraction with detergent, complexes containing His-tagged RGS8 were purified by Ni^{2+}-NTA–agarose. **a**, Proteins bound to RGS8 were resolved by SDS–PAGE and detected by staining with Coomassie brilliant blue. Lanes: 1, purified His-tagged RGS8; 2, recovered His-tagged RGS8 from buffer alone; 3, proteins recovered in the absence of His-tagged RGS8; 4, proteins recovered in the presence of His-tagged RGS8. Position of the 40K protein recovered with His-tagged RGS8 is indicated. **b**, Identification of Gα subunit bound to RGS8. Rat-brain membrane proteins (top) and proteins bound to His-tagged RGS8 (bottom) were analysed by immunoblotting with antibodies against: lane 1, Gαi1 and Gαi2; lane 2, Gαi3; lane 3, Gαz; lane 4, Gαq/11; lane 5, Gαo.

G-protein-coupled inwardly rectifying K^+ channels are activated directly by Gβγ subunits[11] released from pertussis-toxin-sensitive G proteins of the G_i family, including G_i and G_o (ref. 12). They are activated by various G-protein-coupled receptors such as the m2 muscarinic receptor[13], the D2 dopamine receptor[13], metabotropic glutamate receptors[14], the $GABA_B$ receptor[15], and μ and δ opioid receptors[16]. As turning off the G-protein-coupled K^+ channel upon removal of the agonist is much faster than the rate of basal GTP hydrolysis by purified Gα subunits[17], soluble factors like GAP have been proposed to be responsible for this rapid switching off[18].

We co-expressed the brain-type G-protein-coupled inwardly rectifying K^+ channels, GIRK1[19]/GIRK2 heteromultimer[16,20,21] and D2 dopamine receptor (Fig. 4a) or m2 muscarinic receptor (Fig. 4b) with or without RGS8 in *Xenopus* oocytes, and analysed the speed of turning on and off upon agonist application under two-electrode voltage clamp. Co-expression of RGS8 accelerated both turning on and off (Fig. 4a, b). The increasing and decreasing phases were well fitted by a single exponential function, and the time constants for the fit, τ_{on} and τ_{off}, are shown in Fig. 4c. The acceleration of turning on and off by RGS8 were statistically significant. Results were similar when cardiac-type G-protein-coupled inwardly rectifying K^+ channel GIRK1/CIR[22] was used instead of the brain type GIRK1/GIRK2 (data not shown).

How can the acceleration of both the turning on and off of the GIRK current be explained? One possibility is that RGS8 has a dual function: that is, it can act as an off-rate accelerator (GAP) but also as an on-rate accelerator (for example, an accelerator of GDP–GTP exchange or of dissociation of Gα and Gβγ). Another possibility is that RGS8 simply functions as a GAP, and that the time required to reach equilibrium upon receptor activation (1/(on-rate + off-

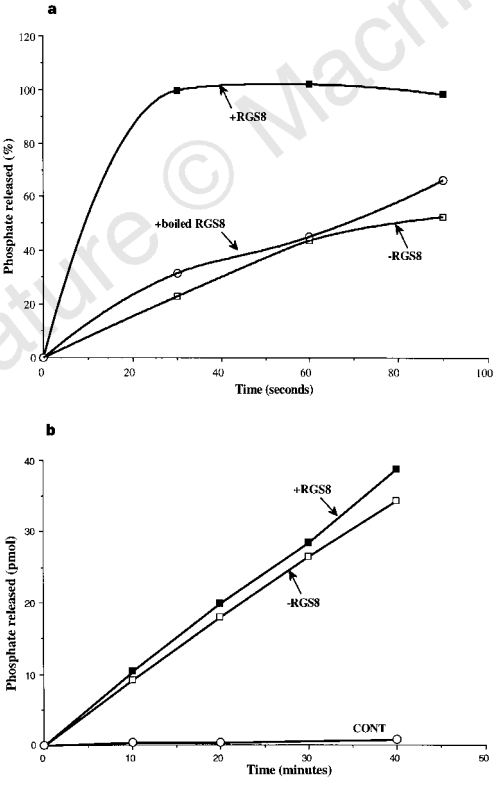

Figure 3 Effects of RGS8 on GTP hydrolysis of Gαo. **a**, The kinetics of GTP hydrolysis during a single catalytic turnover by Gαo alone (open squares) or by Gαo with RGS8 (filled squares) or with boiled RGS8 (circles). Released phosphate is expressed as a percentage of the maximum level (3.3 pmol). **b**, Kinetics of steady-state hydrolysis of GTP by Gαo alone (open squares) or Gαo with RGS8 (filled squares) or buffer (circles). Data are representative of at least two independent experiments.

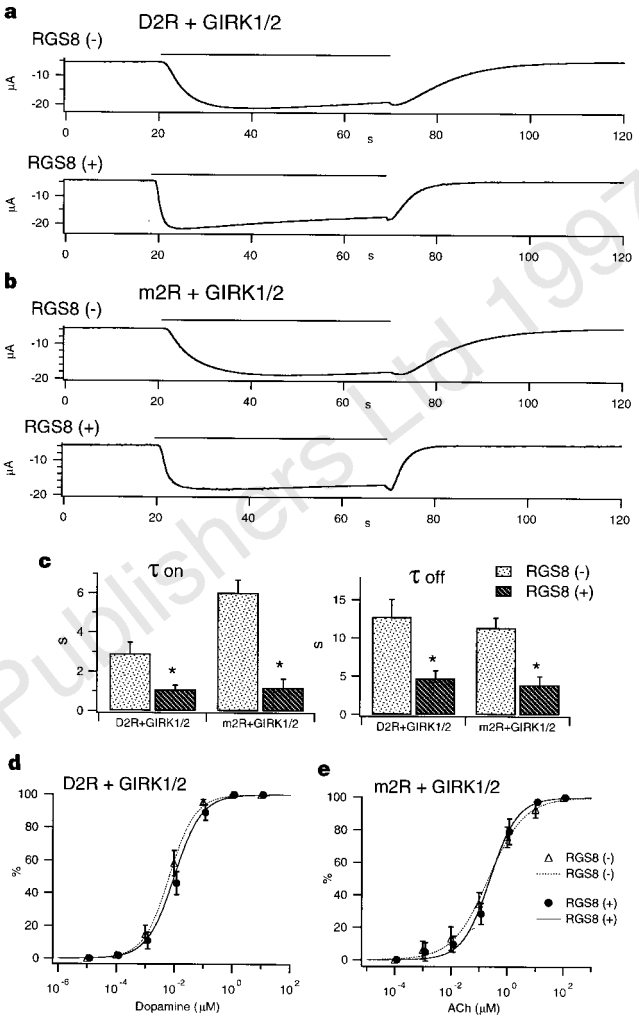

Figure 4 Effects of RGS8 on turning-on and turning-off kinetics, and on the dose–response relationships of the G-protein-coupled inwardly rectifying K^+ channel (GIRK1/2) current upon stimulation of the receptors. **a**, GIRK1/2 and D2 dopamine receptor without (upper trace) or with (lower trace) RGS8 were co-expressed in *Xenopus* oocytes. Current traces at a holding potential of –120 mV are shown. 50 nM dopamine was applied at the time indicated by the bars. The kinetics of the turning on and off are faster for co-expression with RGS8. **b**, Same as in **a**, except that co-expression was with the m2 muscarinic receptor instead of D2 dopamine receptor. ACh (4 μM) was applied at the time indicated by the bars. **c**, Comparison of the time constants τ_{on} and τ_{off} of the GIRK1/2 current upon stimulation of the D2 or m2 receptor, in the absence or presence of RGS8. From the traces in **a** and **b**, the increasing and decreasing phases were fitted by a single exponential function and τ_{on} and τ_{off} were obtained. The mean and standard deviation of τ_{on} ($n = 14$) were: (D2 receptor, RGS(–)); 2,905 ± 576 ms; (D2 receptor, RGS(+)); 1,103 ± 206 ms; (m2 receptor, RGS(–)): 6,021 ± 651 ms; (m2 receptor, RGS(+)): 1,188 ± 444 ms. Those of τ_{off} ($n = 14$) were: (D2 receptor, RGS(–)): 12,761 ± 2,360 ms; (D2 receptor, RGS(+)): 4,714 ± 998 ms; (m2 receptor, RGS(–)): 11,361 ± 1,304 ms; (m2 receptor, RGS(+)): 3,909 ± 1,087 ms. Asterisks indicate data judged to be significantly different from control values (P value < 0.05) by Student's unpaired t-test. **d**, Comparison of dose–response relationships upon stimulation of the D2 receptor in the absence (triangles, broken line) and presence (filled circles, solid line) of RGS8. Responses to all doses were tested in a single oocyte and normalized. The average and s.d. of five oocytes were plotted. K_d values and Hill coefficients for fitting were 6.7 nM, 0.96, respectively, for RGS8(–), and 10 nM, 0.92 for RGS8(+). **e**, Same as in **d**, except that the m2 instead of D2 receptor was used. K_d values and Hill coefficients for fitting were 0.21 μM, 0.68 for RGS8(–), and 0.25 μM, 0.89 for RGS8(+).

rate)) is shortened by the increase in off-rate. If so, the equilibrium should be shifted towards the GDP-bound form. However, the equilibrium was not shifted, because the dose–response relationships (Fig. 4d, e) and the amplitudes of basal and induced currents (data not shown) were not significantly changed by RGS8. Thus our observations cannot all be explained by assuming that RGS8 functions only as a GAP. We therefore propose that RGS8 functions not only as a GAP but also as a on-rate accelerator, for example in promoting GDP–GTP exchange or the dissociation of Gα and Gβγ.

We have isolated a full-length cDNA encoding RGS8, a unique member of the RGS family. Specific features of RGS8 are its expression in the brain and its preferred binding to Gαo and Gαi3. Biochemical reconstitution has revealed that RGS8 acts as a GAP for Gα and functional studies in *Xenopus* oocytes showed that RGS8 significantly accelerates the turning on of the K^+ channel upon addition of agonist, as well as turning off when the agonist is washed out. Although RGS proteins have been proposed to be negative regulators of G-protein-coupled signal transduction[1], our results indicate that they also accelerate the turning-on and -off kinetics of G-protein signalling. As RGS8, Gαo and GIRK1/2 are all expressed in the brain, this accelerated response caused by RGS8 may occur in the brain to enable the resting potential and the firing of neuronal cells to be rapidly regulated.

Note added in proof: Doupnik *et al*. reported similar electrophysiological results on RGS 1, 3, and 4 (*Proc. Natl Acad. Sci. USA* **94,** 10461–10466; 1997). □

Methods

RT-PCR. To identify RGS proteins expressed in neuronally differentiated P19 cells, RT-PCR was used with degenerate primers corresponding to conserved RGS domains as described[3]. Total RNA was isolated from P19 cells differentiated by retinoic acid treatment. The first strand cDNA was synthesized as a template of PCR. The amplified 200-bp DNA was cloned into pGEM-T vector (Promega) and its sequence determined. Three rat RGS proteins, RGS8, RGS2 and RGS-r were identified. Primers specific for these three RGS proteins (RGS8: 5′-AGTTCAAGAAGACCAGGTCAACT-3′, 5′-TTTTCCCTGAGCTTGATCAAAACAA-3′. RGS2: 5′-TTGGCTTGTGAAGACTTCAA-3′, 5′-AAACTGTACACCCTCTTCTGA-3′, RGS-r: AGTTCAAGAAGATCCGATCAGCCA-3′, 5′-ACATCGAAGCAACTGGTAGT-3′) were synthesized and the expression of each RGS was examined by RT-PCR using RNAs isolated from undifferentiated and differentiated P19 cells.

Cloning of cDNA. Rat hippocampus cDNA library (generously provided by K. Yamagata) was screened with the PCR-amplified fragment of RGS8. The longest cDNA clone was sequenced on both strands.

Expression and purification of His-tagged RGS8. RGS8 was expressed as a full-length protein with hexa-histidine tags at the amino terminus. A bacterial expression plasmid of His-tagged RGS8 was constructed as follows. The entire coding region of RGS8 cDNA was used to generate a PCR fragment and the nucleotide sequence of the amplified DNA was confirmed by sequencing both strands. The DNA fragment encoding RGS8 was cloned into the *Bam*HI and *Sma*I sites of pQE30 (Qiagen). The resultant plasmid was transformed into *E. coli*, strain M15. His-tagged RGS8 was induced with 2 mM IPTG for 4 h and extracted by sonication in 50 mM sodium phosphate, pH 7.4, 1.3 M NaCl, 10% glycerol and 40 mM imidazole (sonication buffer). Lysates were clarified by centrifugation and then applied to Ni^{2+}-NTA–agarose (Qiagen) columns. Columns were washed with sonication buffer containing 10 mM β-mercaptoethanol. The proteins were eluted in a stepwise manner with increasing concentrations of imidazole. His-tagged RGS8 was eluted with 0.4 M imidazole.

Binding assay of RGS8. RGS8–G protein binding was assayed as described[6]. His-tagged RGS8 (10 μg) was incubated for 30 min at 5 °C with rat brain membrane fractions (0.5 mg) treated with 10 μM GDP and 30 μM AlF_4^-. After extraction with 1% cholate, complexes containing His-tagged RGS8 isolated with Ni^{2+}-NTA–agarose were examined by SDS–PAGE. Proteins bound to RGS8 were identified by immunoblotting with antibodies against Gαi1 and Gαi2, Gαi3, (Calbiochem-Novabiochem), Gαo, Gαz and Gαq/11 (Santa Cruz Biotechnology). Signals were detected with an ECL system (Amersham). The membrane filters were exposed to X-ray films (Hyperfilm, Amersham) for 2 min to detect Gαo and for 6 min for the other Gα proteins.

Analysis of GTP hydrolysis. Gαo was purified from bovine brain as described[23]. GTPase was assayed as described[5]. To obtain the catalytic rate of GTP hydrolysis, Gαo (0.21 μM) was loaded with 0.55 μM [γ-^{32}P]GTP in 50 mM Na-HEPES (pH 8.0), 2 mM dithiothreitol, 5 mM EDTA and 0.05% C12E10 for 15 min at 20°C, then the temperature was reduced by placing on ice for 5 min. Before initiation of GTP hydrolysis, a 50-μl aliquot of the mixture was removed and added to 750 μl of 5% (w/v) Norit in 50 mM NaH_2PO_4 (0 °C) as the zero time point. Then, unlabelled GTP (166 μM), $MgSO_4$ (16.6 mM), and His-tagged RGS8 (1 μM) or buffer were added to the reaction mixture. Aliquots (50 μl) were taken at the indicated intervals and added to 5% Norit. The charcoal was removed by centrifugation and 400-μl aliquots of supernatant containing $^{32}P_i$ were counted by liquid scintillation spectrometry. To examine steady-state hydrolysis of GTP, Gαo alone (0.24 μM) or Gαo with 0.88 μM His-tagged RGS8 were incubated at 20 °C with 6 mM $MgSO_4$, 1.27 μM [γ-^{32}P]GTP, and 3.2 μM cold GTP in 50 mM NaHEPES (pH 8.0), 1 mM EDTA, 2 mM dithiothreitol, and 0.05% C12E10. Aliquots (50 μl) were removed at the indicated times and processed as described.

Two-electrode voltage clamp. *Xenopus* oocytes were treated with collagenase (2 mg ml^{-1}) for 2 h at room temperature to remove follicle cells and injected with 50 nl of *in vitro* transcribed RNA solution (1 μg μl^{-1}). Electrophysiological recordings were made 2–4 d later at room temperature (23 ± 2 °C) under two-electrode voltage clamp (OC-725B-HV, Warner). Data were acquired and analysed on a 80486-based computer using Digidata 1200 and pCLAMP program (Axon Instruments). Intracellular glass microelectrodes were filled with 3 M KCl; the resistance was 0.2–0.8 M ohm. The bath solution contained 90 mM KCl, 3 mM $MgCl_2$, 20 μM $GdCl_3$, 10 mM HEPES (pH 7.4). Concentrated stock (5×) agonist solution was applied to the bath (20% of bath volume) so that the flow was not directed at the oocytes, and then mixed immediately by pipetting. Rapid perfusion and vacuum suction was used to wash out agonists in the bath. The exchange rate of solutions in the bath was determined by changing the K^+ concentration using the same methods. The value τ_{in} ranged from 299 to 533 ms, and τ_{out} from 840 to 1,132 ms; this speed is sufficient for the accurate analysis of the off-rate. The fast on-rate in the presence of RGS8 is estimated to be slightly slower than the real value. This error does not affect our conclusion that turning on is faster when RGS8 is co-expressed.

Received 29 July; accepted 5 September 1997.

1. Koelle, M. R. A new family of G-protein regulators—the RGS protein. *Curr. Opin. Cell Biol.* **9,** 143–147 (1997).
2. Dohlman, H., Apaniesk, D., Chen, Y., Song, J. & Dlusskem, D. Inhibition of G-protein signaling by dominant gain-of-function mutation in Sst2p, a pheromone desensitization factor in *Saccharomyces cerevisiae*. *Mol. Cell Biol.* **15,** 3635–3643 (1995).
3. Koelle, M. R. & Horvitz, H. R. EGL-10 regulates G protein signaling in the *C. elegans* nervous system and shares a conserved domain with many mammalian proteins. *Cell* **84,** 115–125 (1996).
4. Druey, K. M., Blumer, K. J., Kang, V. H. & Kehrl, J. H. Inhibition of G-protein-mediated MAP kinase activation by a new mammalian gene family. *Nature* **379,** 742–746 (1996).
5. Berman, D. M., Wilkie, T. M. & Gilman, A. G. GAIP and RGS4 are GTPase-activating proteins for the Gi subfamily of G protein α subunits. *Cell* **86,** 445-452 (1996).
6. Watson, N., Linder, M. E., Druey, K. M., Kehrl, J. H. & Blumer, K. J. RGS family members: GTPase-activating proteins for heterotrimeric G-protein α-subunits. *Nature* **383,** 172–175 (1996).
7. Hunt, T. W., Fields, T. A., Casey, P. J. & Peralta, E. G. RGS10 is a selective activator of Gαi GTPase activity. *Nature* **383,** 175–177 (1996).
8. Jones-Villeneuve, E. M. V., McBurney, M. W., Rogers, K. A. & Kalnins, V. I. Retinoic acid induces embryonal carcinoma cells to differentiate into neurons and glial cells. *J. Cell Biol.* **94,** 253–262 (1982).
9. Chen, C.-K., Wieland, T. & Simon, M. I. RGS-r, a retinal specific RGS protein, binds an intermediate conformation of transducin and enhances recycling. *Proc. Natl Acad. Sci. USA* **93,** 12885–12889 (1996).
10. Siderovski, D. P., Heximer, S. P. & Forsdyke, D. R. A human gene encoding a putative basic helix-loop-helix phosphorprotein whose mRNA increases rapidly in cycloheximide-treated blood mononuclear cells. *DNA Cell Biol.* **13,** 125–147 (1994).
11. Reuveny, E. *et al.* Activation of the cloned muscarinic potassium channel by G protein βγ subunits. *Nature* **370,** 143–146 (1994).
12. Wickman, K. & Clapham, D. E. Ion channel regulation by G proteins. *Physiol. Rev.* **75,** 865–885 (1995).
13. Werner, P., Hussy, N., Buell, G., Jones, K. A. & North, R. A. D2, D3, and D4 dopamine receptors coupled to G protein-regulated potassium channels in *Xenopus* oocytes. *Mol. Pharmacol.* **49,** 656–661 (1996).
14. Saugstad, J. A., Segerson, T. P. & Westbrook, G. L. Metabotropic glutamate receptors activate G-protein-coupled inwardly rectifying potassium channels in *Xenopus* oocytes. *J. Neurosci.* **16,** 5979–5985 (1996).
15. Sodickson, D. L. & Bean, B. P. $GABA_B$ receptor-activated inwardly rectifying potassium current in dissociated hippocampal CA3 neurons. *J. Neurosci.* **15,** 6374–6385 (1996).
16. Lesage, F. *et al.* Cloning provides evidence for a family of inward rectifier and G-protein coupled K^+ channels in the brain. *FEBS Lett.* **353,** 37–42 (1994).
17. Breitwieser, G. E. & Szabo, G. Mechanism of muscarinic receptor-induced K^+ channel activation as revealed by hydrolysis-resistant GTP analogues. *J. Gen. Physiol.* **91,** 469–493 (1988).
18. Shui, Z., Boyett, M. R., Zang, W. J., Haga, T. & Kameyama, K. Receptor kinase-dependent desensitization of the muscarinic K^+ current in rat atrial cells. *J. Physiol. (Lond.)* **487,** 359–366 (1995).

19. Kubo, Y., Reuveny, E., Slesinger, P. A., Jan, Y. N. & Jan, L. Y. Primary structure and functional expression of a rat G-protein-coupled muscarinic potassium channel. *Nature* **364,** 802–806 (1993).
20. Lesage, F. *et al.* Molecular properties of neuronal G-protein-activated inwardly rectifying K^+ channels. *J. Biol. Chem.* **270,** 28660–28667 (1995).
21. Velimirovic, B. M., Gordon, E. A., Lim, N. F., Navarro, B. & Clapham, D. E. The K^+ channel inward rectifier subunits form a channel similar to neuronal G protein-gated K^+ channel. *FEBS Lett.* **379,** 31–37 (1996).
22. Krapivinsky, G. *et al.* The G-protein-gated atrial K^+ channel I_{KACh} is a heteromultimer of two inwardly rectifying K^+-channel proteins. *Nature* **374,** 135–141 (1995).
23. Asano, T., Kamiya, N., Morishita, R. & Kato, K. Immunoassay for the βγ subunits of GTP-binding proteins and their regional distribution in bovine brain. *J. Biochem.* **103,** 950–953 (1988).
24. Abe, H., Saitoh, O., Nakata, H., Yoda, A. & Matsuda, R. Expression of neurofilament proteins in proliferating C2C12 mouse skeletal muscle cells. *Exp. Cell Res.* **229,** 48–59 (1996).

Acknowledgements. We thank M. Lazdunski for GIRK2 cDNA, A. Connolly for m2 muscarinic receptor and D2 dopamine receptor cDNA, K. Yamagata for the cDNA library, M. Odagiri for technical assistance. This work is supported by research grants from the Ministry of Education, Science, Sports and Culture of Japan (to O.S.) and from the Human Frontier Science Program Organization (to Y.K.) and by a grant-in-aid for scientific research on priority area of "channel-Transporter Correlation" (to Y.K.).

Correspondence and requests for materials should be addressed to O.S. (e-mail: osaito@tmin.ac.jp) or H.N. (e-mail: nakata@tmin.ac.jp). The nucleotide sequence of rat RGS8 will appear in the DDBJ, EMBL, and GenBank data bases under the accession number AB006013.

Pore-forming segments in voltage-gated chloride channels

Christoph Fahlke, Henry T. Yu, Carol L. Beck, Thomas H. Rhodes & Alfred L. George Jr

Departments of Medicine (Nephrology) and Pharmacology, and the Center for Molecular Neuroscience, Vanderbilt University School of Medicine, Nashville, Tennessee 37232-2372, USA

The ability to differentiate between ions is a property of ion channels that is crucial for their biological functions[1]. However, the fundamental structural features that define anion selectivity and distinguish anion-permeable from cation-permeable channels are poorly understood. Voltage-gated chloride (Cl^-) channels belonging to the ClC family are ubiquitous and have been predicted to play important roles in many diverse physiological[2] and pathophysiological[3–5] processes. We have identified regions of a human skeletal muscle ClC isoform that contribute to formation of its anion-selective conduction pathway. A core structural element (P1 region) of the ClC channel pore spans an accessibility barrier between the internal and external milieu, and contains an evolutionarily conserved sequence motif: GKxGPxxH. Neighbouring sequences in the third and fifth transmembrane segments also contribute to isoform-specific differences in anion selectivity. The conserved motif in the Cl^- channel P1 region may constitute a 'signature' sequence for an anion-selective ion pore by analogy with the homologous GYG sequence that is essential for selectivity in voltage-gated potassium ion (K^+) channel pores[6–8].

All known ClC channels have a conserved motif located at the carboxy-terminal side of transmembrane segment D3 (designated as the P1 region) which in human ClC-1 (hClC-1) has the sequence GKEGPFVH (residues 230–237) (Fig. 1a). A naturally occurring substitution (G230E) in this segment that causes autosomal dominant myotonia congenita (Thomsen's Disease)[9] greatly distorts permeation properties of the channel suggesting that this residue may lie within or near the ion-conduction pathway[10]. To investigate this region in more detail, we made amino-acid substitutions for each residue between Gly 230 and His 237, and evaluated channel function using the patch-clamp technique. Representative whole-cell current recordings and instantaneous current–voltage relationships obtained from each mutant are shown in Fig. 1b. Mutations in P1 affect open-channel rectification and block by extracellular iodide (Fig. 1b, open symbols). Furthermore, all mutations constructed in P1 confer altered anion selectivity on hClC-1 as deduced from permeability ratios (Table 1). Substitutions at positions 230, 231 and 233 have the greatest effect on the anion-selectivity sequence, whereas mutations at 232, 235 and 236 have smaller but significant effects on selectivity. In addition, mutations of Gly 230, Lys 231 and Gly 233 confer increased cation permeability (Table 1). Channel gating was also very sensitive to mutations of residues Gly 230 to Pro 234 as has been reported for pore mutations in voltage-gated K^+ channels[6].

To test whether residues in the P1 region project their side groups into an aqueous cavity, consistent with an ion-conduction pathway, we performed cysteine-scanning mutagenesis and examined the mutants for reactivity to substituted water-soluble methanethiolsulphonates (MTS reagents)[11]. Wild-type hClC-1 exhibits no functional change upon exposure to MTS reagents applied intra- or extracellularly under our experimental conditions (Fig. 2a). A cysteine placed at position 231 is accessible only to extracellularly applied MTS-ethylsulphonate (MTSES), whereas cysteines at positions 234 and 237 are reactive only to intracellularly applied MTSES (Fig. 2a). Application of MTS-ethyltrimethylammonium (MTSET) causes comparable reductions in current amplitudes (data not shown). The functional effects of MTS reagents on cysteine-sub-

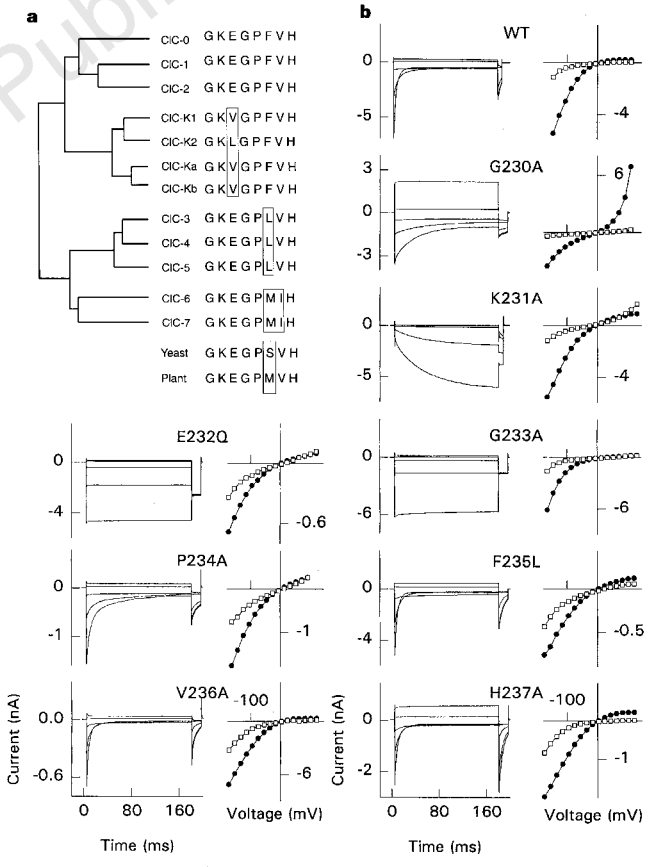

Figure 1 Evolutionary conservation of the GKEGPFVH motif in P1, and the effect of mutations. **a**, Alignment of P1 region in ClC channels. Least-conserved residues are boxed. **b**, Representative current recordings from WT and mutant hClC-1 channels. For each construct, voltage steps between –165 mV and +75 mV in 60-mV steps were applied from a holding potential of 0 mV. Each test pulse is followed by a fixed –105 mV pulse. Whole-cell recordings are shown for: WT, G230A, K231A, E232Q and G233A. Excised inside-out patches were used for: P234A, F235L, V236A, H237A. Instantaneous current–voltage relationships were measured after a 250 ms prepulse to +75 mV (–100 mV for K231A) in standard extracellular solution (filled circles) and for the same cell/patch after changing to (in mM): NaI (140), KCl (4), $CaCl_2$ (2), $MgCl_2$ (1), HEPES (5) (open squares). Whole-cell recordings are shown for: WT, G230A, K231A, G233A. Excised outside-out patches for: E232Q, P234A, F235L, V236A, H237A.